Icarus 255 (2015) 3–17

Contents lists available at ScienceDirect

Icarus

journal homepage: www.elsevier.com/locate/icarus

Simultaneous analysis of abundance and isotopic composition of nitrogen, carbon, and noble gases in lunar basalts: Insights into interior and surface processes on the Moon

J. Mortimer [a], A.B. Verchovsky [a], M. Anand [a,b,*], I. Gilmour [a], C.T. Pillinger [a,1]

[a] Planetary and Space Sciences, Department of Physical Sciences, The Open University, Milton Keynes MK7 6AA, UK
[b] Department of Earth Sciences, Natural History Museum, Cromwell Road, London SW7 5BD, UK

ARTICLE INFO

Article history:
Received 29 January 2014
Revised 1 October 2014
Accepted 5 October 2014
Available online 19 October 2014

Keywords:
Moon, interior
Moon, surface
Cosmochemistry

ABSTRACT

Simultaneous static-mode mass spectrometric measurements of nitrogen, carbon, helium, neon, and argon extracted from the same aliquot of sample by high-resolution stepped combustion have been made for a suite of six lunar basalts.

Collecting abundance and isotopic data for several elements simultaneously from the same sample aliquot enables more detailed identification of different volatile components present in the basalts by comparing release patterns for volatiles across a range of temperature steps. This approach has yielded new data, from which new insights can be gained regarding the indigenous volatile inventory of the Moon.

By taking into account N and C data for mid-temperature steps, unaffected by terrestrial contamination or cosmogenic additions, it is possible to determine the indigenous N and C signatures of the lunar basalts. With an average $\delta^{15}N$ value of around +0.35‰, the indigenous N component seen in these samples is similar within error to other (albeit limited in number) isotopic measurements of indigenous lunar N. Average C/N ratios for indigenous volatiles in these six basalt samples are much lower than those of the terrestrial depleted mantle, or bulk silicate Earth, possibly suggesting much less C in the lunar interior, relative to N, than on Earth.

Cosmogenic isotopes in these samples are well-correlated with published sample exposure ages, and record the rate of *in situ* production of spallogenic volatiles within material on the lunar surface.

1. Introduction

In recent years, the search for lunar volatiles has attracted renewed interest; new analyses of lunar glasses and apatite crystals suggest initial magma volatile contents (mainly H, reported as either OH or H_2O) many times higher than previously reported (e.g., Füri et al., 2014; Greenwood et al., 2011; McCubbin et al., 2010; Saal et al., 2008; Tartèse et al., 2013), some with terrestrial-like volatile abundances (e.g., Boyce et al., 2010; Hauri et al., 2011).

In light of these new data, and given the advances in analytical techniques made in the decades since the Apollo missions returned lunar samples to Earth, it is timely to reassess some other light volatile elements (C, N) and noble gases (He, Ne, Ar) in lunar samples, to constrain better their origin(s) and abundances.

Mare basalts provide an important window into the lunar interior, yielding data about the material from which the Earth–Moon system formed, and about the early geochemical evolution of the Moon. Crucially, mare basalts (and associated pyroclastic glasses) are derived from the lunar mantle, and thus comprise a key sample set from which the indigenous volatile inventory of the lunar interior can be assessed. Furthermore, post-emplacement history of mare basalts also provide a record of cosmogenic volatiles produced at the surface of the Moon over time, in addition to the indigenous lunar volatile components locked into the basalts at crystallisation.

Stepped heating techniques have been used in analyses of lunar samples since the early 1970s, when the Apollo samples were first returned to Earth (e.g. Friedman et al., 1970), and so are well-established analytical methods for use with extra-terrestrial material.

For stepped combustion analyses, such as those presented in this paper, each lunar sample is incrementally heated in the presence of oxygen gas. As a sample is heated, the release patterns of

* Corresponding author at: Planetary and Space Sciences, Department of Physical Sciences, The Open University, Milton Keynes MK7 6AA, UK.
E-mail address: Mahesh.Anand@open.ac.uk (M. Anand).
[1] Deceased.

http://dx.doi.org/10.1016/j.icarus.2014.10.006
0019-1035/

the combustion products of carbon (CO_2) and the gases released by pyrolysis (N_2 and noble gases) are recorded; the isotopic compositions of all the gases are measured at each temperature step. This enables different components present in the sample, which are associated with different release temperatures and isotopic signatures, to be distinguished from one another.

Crucial for the study of extra-terrestrial material, such as the lunar samples, is the capability of this method to distinguish the abundance and isotopic signature of terrestrial contaminants, which are more labile components and released at lower temperatures, from any indigenous lunar volatile components released at higher temperatures. In a single-step combustion analysis, in which the entire sample is combusted at the same high-temperature, these components from different sources are not resolvable.

Stepped combustion experiments on mare basalt samples have been carried out by a number of groups over the last four decades, although not all of these studies collected isotopic data (Table 1 contains a list of some previous lunar basalt studies, which focus mainly on N, C, and He, some of which employed stepped combustion techniques, and others which used different methods). However, it is worth noting that even those studies using stepped heating methods were of limited resolution, typically collecting data in only a small number of steps across the temperature range.

In this new study, we combine higher resolution (multiple steps, down to 50 °C intervals), with simultaneous collection of data for more element and isotope systems (N, C, He, Ne, and Ar) at each step, all from the same aliquot of lunar sample. Therefore, this new dataset represents a comprehensive, detailed inventory of volatiles in lunar basalts, building on and augmenting the results of previous studies.

2. Samples

For this study, six Apollo basalt samples were selected (Table 2), covering a range of crystallisation ages, cosmic ray exposure ages, and compositional variations (both high Ti and low Ti basalts). These samples cover all of the US sample return missions, apart from Apollo 16 which mainly sampled lunar highlands anorthositic rocks, rather than the mare basalts which are the focus of this work.

A second aliquot of 12064,138 (Run 2) was analysed for Ne approximately 6 months after the first aliquot (Run 1), for the purposes of confirming the Ne isotope ratio mixing trend observed in the first run (see Section 5.4.3 for further discussion).

3. Methods

Approximately 250 mg of a single chip of each mare basalt was crushed using an agate mortar and pestle, to produce a homogenous powder, necessary for sub-sampling; around 5 mg samples were used for stepped-combustion analysis. In order to minimise any terrestrial contamination of the samples before analysis, the basalt powders were weighed out and transferred into 4 mm × 4 mm clean platinum foil buckets in a Class 100 clean room (Pt foil cleaning methods are as described in Abernethy et al., 2013). Tweezers and spatulas used to transfer the basalt powders from their respective vials to the platinum buckets were cleaned before use, and wiped with acetone using lint-free cloths between uses with separate samples.

The 'Finesse' mass spectrometric instrument used in this study is a custom-built mass spectrometer system, consisting of three dedicated static-mode mass spectrometers (one for carbon, one for nitrogen and argon, and a quadrupole for helium and neon), all linked *via* high vacuum lines to a common sample inlet and combustion furnace (see Wright et al., 1988; Wright and Pillinger, 1989; Verchovsky et al., 1997 for further details, and Boyd et al., 1997, for a review of the stepped-heating method).

Samples were combusted in oxygen, supplied from CuO, in a double-walled quartz-ceramic furnace for 30 min at each temperature step, followed by 15 min for oxygen resorption, before transfer of the gases produced to the clean-up section. For the initial batch of samples, only thirteen combustion steps were used, in 100 °C steps from 200 to 1400 °C. However, for the final three samples (12040, 12064 (Run 2), and 15555), a total of seventeen combustion steps were employed to acquire higher-resolution data across the mid-range temperatures, heating in 100 °C steps from 200 to 600 °C, then in 50 °C steps from 650 to 950 °C, followed by 100 °C steps from 1000 to 1400 °C. Gas fractions were cryogenically separated using liquid nitrogen cooled traps, some of which were filled with molecular sieves. Argon and neon were purified using Ti–Al getters, and nitrogen was purified using a CuO furnace to ensure no CO was present. Carbon yields (recorded as ng of C) were calculated using the pressure of CO_2 measured on a calibrated MKS Baratron™ capacitance manometer. Nitrogen yields (also recorded as ng) were measured *via* calibration of the mass spectrometer ion current at $m/z = 28$, with yields of noble gases also determined by calibration of mass spectrometer peak intensities at the appropriate m/z values. Gases were transferred to different

Table 1
Previous nitrogen, carbon, and noble gas analyses of lunar basalts. Sample numbers in bold refer to samples used in common with this study.

Author(s)	Year	Lunar basalt sample(s)	Volatiles	Method
Des Marais	1978	15058, **15555**, 70215, 75035	$\delta^{13}C_{(VPDB)}$, $\delta^{15}N_{(AIR)}$	Stepped combustion at 420 °C, 500 °C, and 1230 °C (varies between samples)
	1983	15016, 15058, 15499, **15555**, 70017, 74275	$\delta^{13}C_{(VPDB)}$, $\delta^{15}N_{(AIR)}$	Stepped combustion at 420 °C, 500 °C, and 1230 °C (varies between samples)
Friedman et al.	1970	**10017**	$\delta^{13}C_{(VPDB)}$	Combustion to 1350 °C
	1971	12004, 12021, 12051	$\delta^{13}C_{(VPDB)}$	Combustion to 900 °C
	1972	**15555**	$\delta^{13}C_{(VPDB)}$	Combustion to 950 °C
Gibson and Andrawes	1978	15058, 15065, 15499, 15556, 70215, 74255, 74275, 75035, 78505	N (abundance only)	Crushing
Gibson and Johnson	1971	**10017**, 12022	C, N (abundance only)	Thermal gas release
Kaplan et al.	1976	15016, 15499, **15555**	$\delta^{13}C_{(VPDB)}$, $\delta^{15}N_{(AIR)}$, He	Combustion
Mathew and Marti	2001	75075	$\delta^{15}N_{(AIR)}$	Combustion at 400 °C, then stepped pyrolysis up to 1600 °C
Moore et al.	1970	10049, 10050	C, N (abundance only)	Combustion at 1600 °C
	1971	12002, 12022, **12040**, 12044, 12052, 12063, 12065	C, N (abundance only)	Combustion at 1600 °C
	1972	14310	C, N (abundance only)	Combustion at 1600 °C
	1973	15058, 15065, 15076, 15499, 15556, 15595	C (abundance only)	Combustion at 1600 °C
	1974	70215, 71055, 75035	C (abundance only)	Combustion at 1600 °C
Petrowski et al.	1974	70017, 70215, 74275, 75035, 75075	$\delta^{13}C_{(VPDB)}$, $\delta^{15}N_{(AIR)}$, He	Pyrolysis-combustion

Table 2
Summary of samples used in this study.

Sample	Weight (mg)	Crystallisation age	Cosmic ray exposure age	Brief description
10017,342	4.670	3.6 ± 0.215 Ga[a]	480 ± 25 Ma[b]	High Ti and high K fine-grained, vesicular, ilmenite basalt
12040,206	4.656	3.21 ± 0.1 Ga[f]	285 ± 50 Ma[e]	Holocrystalline, coarse-grained olivine basalt
12064,138	Run 1: 5.528 Run 2: 6.357	3.18 ± 0.01 Ga[c]	255 Ma[c], 190–220 Ma[d]	Coarse-grained ilmenite basalt
14053,260	5.395	3.94 ± 0.04 Ga[g]	21 ± 5 Ma[h]	Ophitic Al-rich basalt
15555,982	4.662	3.32 ± 0.06 Ga[i]	81 Ma[j]	Coarse-grained, porphyritic, vuggy olivine basalt
70035,194	5.330	3.82 ± 0.06 Ga[k]	95–100 Ma[g]	High Ti, vesicular, medium-grained ilmenite basalt

[a] Gopalan et al. (1970).
[b] Eberhardt et al. (1974).
[c] Horn et al. (1975).
[d] Hintenberger et al. (1971).
[e] Burnett et al. (1975).
[f] Compston et al. (1971).
[g] Stettler et al. (1973).
[h] Husain et al. (1972).
[i] Wasserburg and Papanastassiou (1971).
[j] Marti and Lightner (1972).
[k] Evensen et al. (1973).

parts of the machine using a system of computer-controlled pneumatic valves. For each temperature step, the isotopes of C, N, He, Ne, and Ar were measured sequentially, taking approximately 1.5 h to complete the cycle for five elements. Once all measurements were complete, the high vacuum line was pumped before the next temperature step.

In order to reduce the contributions from CO_2^{++} and $^{40}Ar^{++}$ on Ne masses (22 and 20), a low ionisation voltage of ~40 V was used in the quadrupole ion source. Also, Ar present in the system was cooled down on the molecular sieves and the Ti–Al getter was open to the mass spectrometer chamber during Ne measurements.

Isotopic data are expressed using the delta (δ) notation, as parts per thousand (‰) deviations from standards (Vienna Peedee Belemnite (VPDB) for C, and terrestrial air (AIR) for N). System blanks were monitored between sample analyses by putting an empty clean Pt foil bucket through the same stepped combustion procedure used for the lunar samples and collecting both abundance and isotopic data. Typical system blank levels were <10 ng C and <1 ng of N. Typical system blanks for ^{4}He were <1E−7 cc, for ^{20}Ne were <6.5E−10 cc, and for ^{40}Ar and ^{36}Ar were <8E−9 cc and <1.2E−10, respectively. All data presented in this paper have been corrected for the contribution of system blanks (unless otherwise stated), and any isotopic averages presented are calculated as weighted averages.

4. Results

4.1. Nitrogen

The stepped combustion results for nitrogen abundance and isotopic composition of the six mare basalts are listed in Table A1 and displayed in Fig. 1. All of the samples display the same general release profiles, with 67–84% of the nitrogen being released at temperatures below 500 °C, most likely associated with terrestrial contamination. Between 15% and 26% of the N present is released at mid-temperature steps (between 600 °C and 900–1000 °C, the exact temperature range varying slightly between samples), and minor amounts (blank level to 17% of the total N present in the samples) are released at high temperatures, typically above 1000–1100 °C, which in all samples are associated with a significant enrichment in ^{15}N at these temperature steps.

4.2. Carbon

The stepped combustion results for carbon abundance and isotopic composition of the six mare basalts are listed in Table A2 and are displayed in Fig. 2. As with nitrogen, the six samples show similar carbon release patterns. In each sample, the majority (51–98%) of the carbon present is released below 600 °C, most likely associated with terrestrial contaminants, with variable δ^{13}C isotopic signatures. Between 1% and 3% of the carbon present is released from the samples at mid-temperature steps (typically between 650 °C and 900–1000 °C), apart from sample 15555, which releases 35% of the total carbon present in the sample between 650 °C and 950 °C. In the high temperature combustion steps (typically above 900–1000 °C), very low amounts of carbon (<1%) are released above the system blank levels in most of the samples, and are associated with ^{13}C-enriched isotopic signatures.

However, in basalts 15555 and 70035 there is a small high-temperature release of carbon at 1000–1200 °C (between 3% and 5% of the total carbon released from these samples, respectively), which is relatively ^{13}C-depleted compared to the other high temperature carbon isotope measurements made for both the same, and the other four, samples.

4.3. Noble gases

The stepped combustion results for noble gases are provided in Tables A3, A4 and A6 (for He, Ne, and Ar, respectively). Ne isotope ratios have been corrected for mass fractionation in the quadrupole mass spectrometer during analyses and for the contribution of a terrestrial atmospheric blank (Table A5). For most of the samples (except 12064,138) the Ne content was so low that its isotopic composition could not be measured with any reasonable precision due to a high contribution of doubly charged CO_2 at ^{22}Ne. In these cases only amounts of ^{21}Ne (cosmogenic) and ^{20}Ne (trapped) have been calculated using the raw data by applying blank corrections for each isotope separately for each temperature step. For that, we used the release pattern of ^{21}Ne and ^{20}Ne, taking the data points outside the release peaks for the isotopes as the blank. Then the temperature steps with the blank level amounts were fitted with a linear of polynomial fit in order to interpolate the data for the temperature steps where the peaks of ^{21}Ne and ^{20}Ne are observed. The ^{21}Ne/^{20}Ne ratio has been used to take into account the contribution of $^{21}Ne_{trapped}$ in order to calculate amounts of $^{21}Ne_{cosmogenic}$. The Ne concentration in sample 12064,138 turned out to be high enough in order to measure its isotopic composition and correct it for the blank contribution, since the contribution from doubly charged CO_2 was almost negligible (mass interference due to the presence of doubly charged CO_2 only became significant when the 44/22 ratio

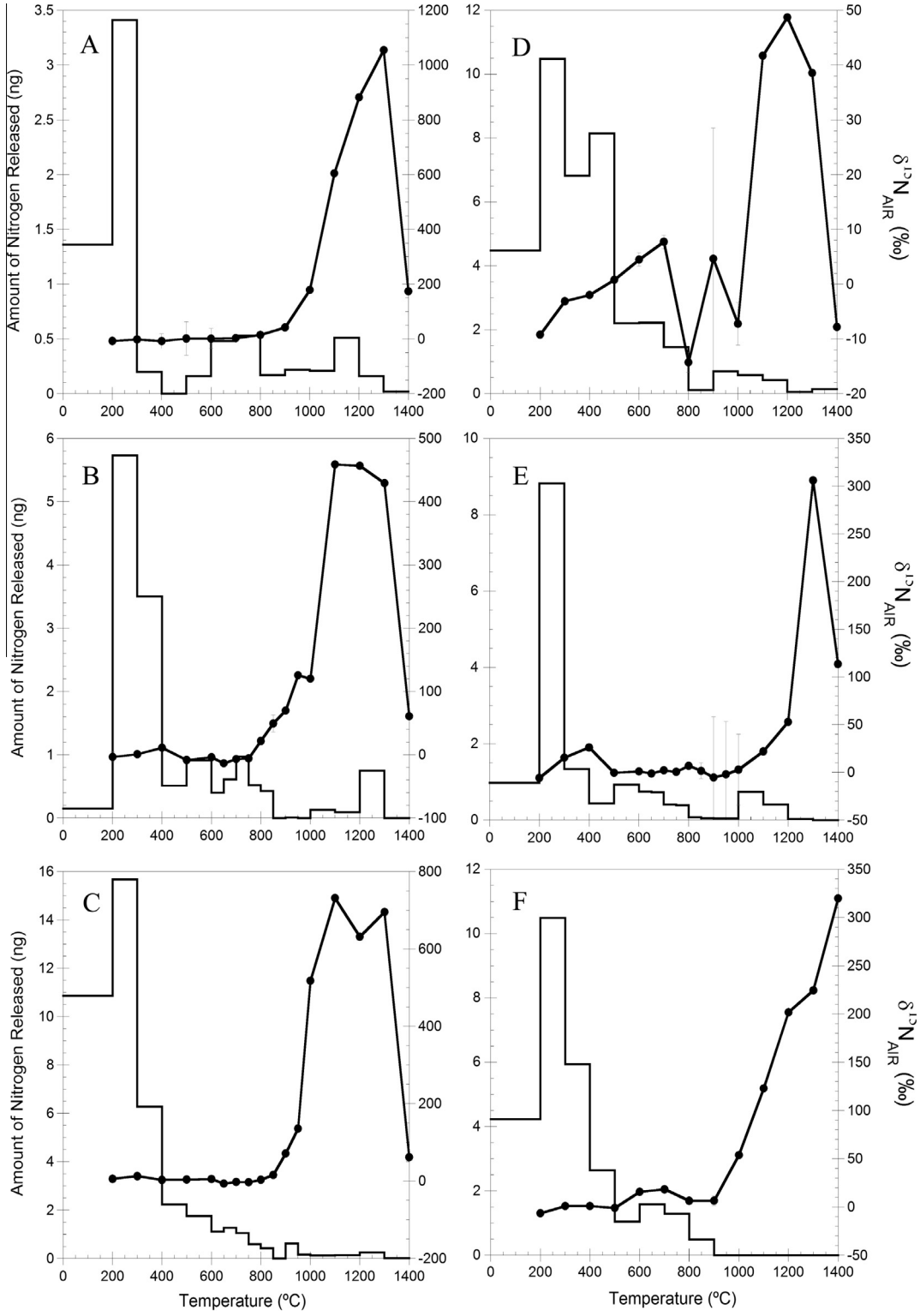

Fig. 1. Stepped combustion profiles of lunar basalts, where A = 10017, B = 12040, C = 12064, D = 14053, E = 15555, and F = 70035. The bar chart represents the amount of nitrogen released at each step (left axis), and the line with dots represents the isotopic $\delta^{15}N$ signature of nitrogen released at each step (right axis). N.B.: each plot uses different scales for both the left and right axes.

was $\geqslant$100; in both analyses of 12064,138, the 44/22 ratio was $\leqslant$50). Blank corrections for ^{4}He, ^{36}Ar and ^{40}Ar have been made in the same manner. He, Ne, and Ar were not measured in basalt 10017. Three different noble gas components have been detected in these samples: cosmogenic ^{21}Ne, radiogenic ^{4}He and ^{40}Ar, and trapped ^{20}Ne and ^{36}Ar.

5. Discussion

5.1. Nitrogen

The release of terrestrial nitrogen from the samples at temperatures below 500 °C is associated with variable $\delta^{15}N$ values (rang-

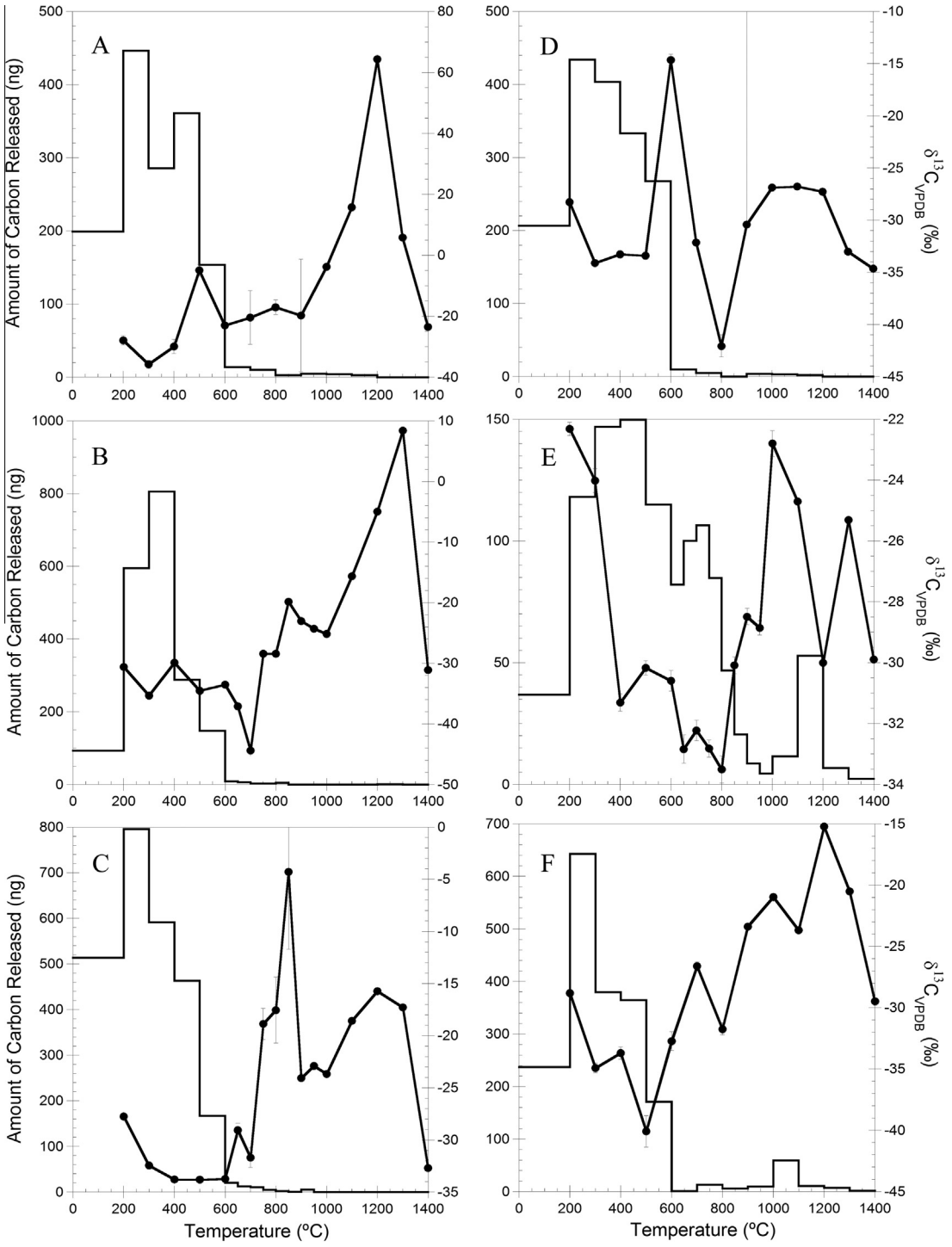

Fig. 2. Results for carbon released by stepped combustion of lunar basalts, where A = 10017, B = 12040, C = 12064, D = 14053, E = 15555, and F = 70035. The bar chart represents the amount of carbon released at each step (left axis), and the line with dots represents the isotopic signature of carbon released at each step (right axis). N.B.: each plot uses different scales for both the left and right axes.

ing from −9.2‰ to +26.2‰). At the highest temperatures, very low amounts of nitrogen are released with a very distinct isotopic signature, extremely ^{15}N-enriched. This suggests that at high temperatures, nitrogen release is dominated by a cosmogenic N component (cosmogenic nitrogen containing a high proportion of ^{15}N relative to ^{14}N). The most ^{15}N-enriched signature measured was +1054.8‰ in sample 10017; this basalt also has the highest calculated exposure age on the lunar surface, at 480 Ma (Table 2). Conversely, the least ^{15}N-enriched high temperature step with a cosmogenic δ^{15}N signature (+48.7‰) was measured in the sample with the lowest exposure age, basalt 14053 at 21 Ma (Table 2).

Because terrestrial contaminants mask any indigenous N signature at low temperature steps, and cosmogenic N components dominate the higher temperature steps, the mid-temperature range (variable between different samples, based on analysis of each sample's individual release profiles, but typically between 650–700 °C to 1000–1100 °C) offers the best opportunity to measure the isotopic signature of any indigenous N present in

the basalt samples. For the six basalts analysed in this study, $\delta^{15}N$ values in the mid temperature range varied between samples, from a maximum of +8.3‰, down to −2.0‰) (Table 3). This small release (typically between 0.5 and 4.5 ng of N) is attributed to a minor indigenous N component in lunar basalts. This range of indigenous $\delta^{15}N$ values, although quite broad, yields a weighted average value of +0.35‰ (±9.11‰ (2σ)), which is slightly lower than previous measurements. However, three of the samples in this study (10017, 15555, and 70035 (Table 3)) have $\delta^{15}N$ values similar (within error) to an indigenous lunar signature of +13.0 ± 1.2‰ across the same temperature range, as measured by Mathew and Marti (2001). A $\delta^{15}N$ value of ~+13‰ has also been reported by Becker et al. (1976), Kerridge et al. (1991) and Murty and Goswami (1992). However, given the range of abundances and $\delta^{15}N$ values measured in just the six samples analysed in this study, it appears that N within the Moon is both heterogeneously distributed, and also isotopically heterogeneous, perhaps as a result of differing amounts of degassing associated with individual mare basalt emplacement events.

5.2. Carbon

The release of terrestrial carbon dominates the low temperature steps up to 600 °C, with variable isotopic signatures of between −4.9‰ and −40.1‰, yielding an average $\delta^{13}C$ value of −27.9‰ across all the samples. In most samples, the amount of carbon being released drops off rapidly in the mid-temperature range (650 °C to 950–1000 °C). However, in 15555, there is an obvious release of a separate C component; the mid-temperature C being released is almost as abundant as the release of low temperature terrestrial C in the same sample. In this sample, the release is associated with an isotopic signature of −33‰, which is more ^{13}C-depleted than both the low-temperature components released from the same sample, and the high temperature component released afterwards.

As with nitrogen, in high-temperature combustion steps, very low amounts of C are released above system blank levels. Cosmogenic carbon, characterised by the high-temperature enrichment in ^{13}C, can be recognised with certainty in 5 samples. For samples 15555 and 70035 there is a very slight increase in the amount of C released between 1000 and 1200 °C. This high-temperature component is present in similar amounts in both samples, and seems to be associated with a slight depletion in ^{13}C, compared to the other, much smaller, high-temperature carbon releases in both the same and other samples analysed. This suggests that it is not purely cosmogenic in origin, and may represent an indigenous high-temperature component which partially masks the ^{13}C-enriched cosmogenic C contribution in these combustion steps in 70035, and completely masks the ^{13}C-enriched cosmogenic component in 15555.

5.3. Indigenous lunar N and C

Using the stepped combustion method, it is possible to identify the temperature ranges where indigenous lunar volatile signatures are overprinted by terrestrial contamination, and an extra-lunar addition from cosmogenic spallation processes. This leaves a 'window' at mid temperatures (typically between 650–700 °C and 1000–1100 °C) where it is feasible to quantify the amount and isotopic composition of indigenous volatile components in lunar basalts.

By comparing the release profiles of C and N in the six basalt samples studied, it is possible to identify several samples where the C and N are most likely co-located in the same phase, although the exact nature of this phase remains unidentified on the basis of release temperature alone. Since C and N do seem to be located in the same phase, it is possible to use the calculated C/N ratios for these indigenous volatile components (released at mid temperatures) as a means of characterising the C and N properties of the lunar mantle, from which these samples are derived. However, degassing during magma eruption and emplacement on the lunar surface may have caused some degree of elemental fractionation, modifying the true lunar mantle ratio, and, therefore, a range of lunar mantle C/N ratios may be expected (discussed in greater detail later in this section).

Table 3
Indigenous lunar nitrogen abundances and isotopic compositions for the six samples analysed in this study. Individual sample errors are weighted averages of propagated errors. Error for the weighted average isotopic composition is 2σ.

Sample	Indigenous N (ng)	$\delta^{15}N$ (‰)	Error (±‰)
10017	1.17	+8.33	12.14
12040	3.84	−2.04	3.76
12064	4.44	−0.75	1.27
14053	4.50	−1.82	2.43
15555	0.60	+4.41	14.25
70035	1.78	+6.53	2.96
Average		+0.35	9.11 (2σ)

The average blank-corrected C/N ratios of the mid temperature indigenous components (Table 4) for five out of the six samples analysed are relatively tightly constrained, between 6 and 21. The exception to this is sample 15555, which has a higher C/N ratio of 49 probably due to the greater release of low temperature carbon contamination still being released at mid-temperature steps in this sample. Since this extra C release is not associated with N, the ratio of C to N increases. Future analysis of sample 15555, preferably using a bulk-rock chip, is needed to gain further insights into the mid-temperature C data acquired in this study. Even after including the data for sample 15555, the variation in average C/N ratios measured among all the six basalts in this study, over the temperature interval interpreted as representing indigenous volatile components, is much smaller than those measured for the terrestrial depleted mantle (C/N_{mantle} = 535 ± 224 (Halliday, 2013; Marty, 2012)), or even for bulk silicate Earth (BSE) (C/N_{BSE} = ~40–50 (calculated from data in Halliday, 2013)).

The large difference in average C/N ratios between the terrestrial depleted mantle and indigenous lunar values may be explained by the significant influence of subducted biological organics greatly increasing the C content of the Earth's mantle relative to N, compared to that of the Moon. Without active plate tectonics, any C added from extra-lunar sources or processes remains

Table 4
C/N ratios of mid-temperature indigenous lunar C and N. N.B. basalt 15555 has a higher C/N ratio than the other samples in this study (see text for further discussion).

Sample	C/N ratio	$\delta^{15}N$ (‰)
10017	21	+8.33 ± 12.14
12040	6	−2.04 ± 2.51
12064	10	−0.75 ± 1.27
14053	4	−1.82 ± 2.43
15555	49	+4.41 ± 14.25
70035	11	+6.53 ± 2.96
Lunar average	**17**	**+0.35 ± 9.11**
Terrestrial depleted mantle	535 ± 224[a]	−5 to −30[c]
Enstatite chondrites	4.5 to 15[b]	−29.2 ± 0.6[b]
CI chondrites	16[d]	~+33[c]
CM chondrites	24[d]	~+50 to +15[c]
CO chondrites	14[d]	~+12 to −20[c]

[a] Taken from Marty and Zimmermann (1999).
[b] Calculated from data in Wasson and Kallemeyn (1988) and Thiemens and Clayton (1983).
[c] Taken and calculated from Marty (2012).
[d] Calculated from average C and N abundances in Pearson et al. (2006).

at the lunar surface, and is not incorporated into the lunar mantle, from which these basalt samples were derived. Therefore, a more relevant comparison might be made between primordial terrestrial mantle C and N values and this indigenous lunar C and N data, although no direct measurements of the primordial terrestrial mantle are available.

Taking an enstatite chondrite composition as a proxy for the primordial terrestrial mantle (Javoy et al., 2010), and using carbon values averaging 3800 ppm (Wasson and Kallemeyn, 1988) and the extremes of the nitrogen values proposed by Thiemens and Clayton (1983) (254–850 ppm), a C/N ratio of between 4.5 and 15 is obtained. Both of these C/N ratios for enstatite chondrites fall within or very close to the range found in this study for indigenous C and N in lunar basalts. However, there is a difference between the indigenous $\delta^{15}N$ signatures for these lunar basalts, and the values measured for enstatite chondrites ($-29.2 \pm 0.6‰$ (Thiemens and Clayton, 1983)), suggesting that indigenous lunar N does not share a common source with that of enstatite chondrites.

Considering carbonaceous chondrites as a possible source for volatiles in the Earth–Moon system (e.g. Marty, 2012), CI and CM chondrites have elemental C/N ratios within/similar to the range calculated for lunar samples. However, N isotopic signatures for these two primitive chondrite groups are heavier than lunar values (Table 4), with an average of around +40‰. CO chondrites, by contrast, not only have C/N ratios within the same range as lunar samples, but also have comparable $\delta^{15}N$ values, supporting the theory that volatiles in the Earth and lunar interior may have a carbonaceous chondrite heritage (e.g. Saal et al., 2013).

A complicating factor regarding the use of C/N ratios is the varying solubility of both C and N between different Solar System bodies, which can have an impact on the C/N elemental ratios measured in mantle samples. Within the Earth, CO_2 solubility is much greater than that of N_2, and hence during degassing, C/N ratios can greatly increase in the residual melt (Cartigny et al., 2001), giving rise to the much higher C/N ratios for the terrestrial mantle as listed in Table 4. Because of this link between solubility and elemental fractionation, the degree of elemental fractionation depends on the speciation of C and N within the mantle melts. Thus, in the lunar mantle, under much more reducing conditions than in the terrestrial mantle, N solubility is greatly increased due to dissolution into the melt as N^{3-} species, which then bond with atoms in the silicate melt network (Libourel et al., 2003). At the same time, under reducing conditions (fO_2 lower than -0.55 relative to the iron wustite buffer), carbon dissolves in the melt as Fe-pentacarbonyl and (to a lesser degree) methane. This change in speciation (from dissolving as carbonate under oxidising conditions) decreases carbon solubility by a factor of two (Wetzel et al., 2013). Therefore, under the reducing conditions of the lunar mantle, carbon is preferentially degassed compared to nitrogen, and this has the effect of decreasing elemental C/N ratios in the residual melts from which lunar mare basalts were formed. These differences between C and N solubilities in the lunar and terrestrial mantles may also explain the observed disparity between elemental C/N ratios in these two bodies.

5.4. Noble gases

5.4.1. Radiogenic noble gas isotopes

Radiogenic ^4He is found in all of the basalts for which helium data were collected. In every sample, the peak release is at 500 °C. Radiogenic ^{40}Ar is also released from the basalt samples across a wide temperature range, but with peak releases between 600 and 700 °C, the slightly higher release temperature for ^{40}Ar being a function of the slower diffusion rate of the larger Ar atom compared to that of He (Fig. 3).

It is worth noting that the actual amounts of radiogenic He and Ar vary across the samples; ^4He and ^{40}Ar are formed *in situ* by the radioactive decay of U and Th, and K, respectively. Because of a correlation between the known chemical compositions of the samples with radiogenic isotope abundances, we can expect samples of the same age with greater initial U and Th, and K to release greater abundances of radiogenic ^4He and ^{40}Ar.

Using literature values, sample 14053 has the highest K abundance, at ~0.11 wt.% (Hubbard et al., 1972) and based on the results of this study, it also releases the most ^{40}Ar (Table A5). 10017 contains more K (Gast et al., 1970), but no Ar data were collected for this sample in this study. Conversely, basalt 15555 has the lowest K content of the samples at ~0.04 wt.% (Chappell and Green, 1973), corresponding with the lowest ^{40}Ar value measured in this study.

The abundances of radiogenic He and Ar are also related to the formation age of their host rocks. The sample which releases the most ^{40}Ar (totalled across all temperature steps) is 14053, with a crystallisation age of 3.94 Ga (Stettler et al., 1973). By comparison, the 2 samples with the lowest ^{40}Ar releases (12040 and 15555) have younger crystallisation ages of 3.21 Ga (Compston et al., 1971) and 3.32 Ga (Wasserburg and Papanastassiou, 1971), respectively.

Besides these expected correlations between released ^{40}Ar abundance, sample composition (K abundance) and crystallisation ages for the samples analysed in this study, comparisons with previously published values from different laboratories show a close agreement in the case of ^{40}Ar, and a good general agreement for ^4He values, demonstrating the effectiveness of the extraction technique used in this study.

5.4.2. Cosmogenic noble gas isotopes

In addition to cosmogenic N and C, cosmogenic ^{21}Ne is also released from all the basalt samples. As with cosmogenic N, ^{21}Ne is well-correlated with published calculated exposure ages for lunar basalts (Fig. 4). For example, Hintenberger et al. (1971) measured 3.13E−7 cc/g^{-1} of cosmogenic ^{21}Ne being released from 12064, from which they calculated a cosmic ray exposure (CRE) age of 220 Ma for the sample. By comparison, analyses performed

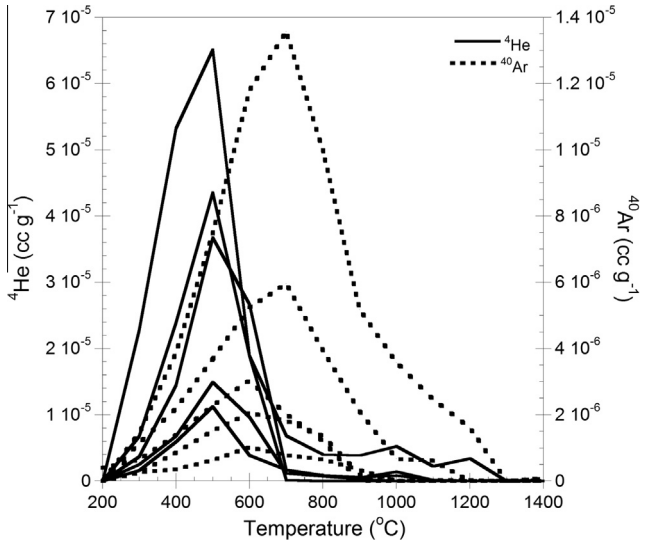

Fig. 3. Radiogenic ^4He and ^{40}Ar release profiles for all basalt samples. Although the amounts of ^4He and ^{40}Ar vary between samples (as a function of initial parent isotope abundances), in each sample, ^4He is released first, at the lower temperature of 500 °C, with ^{40}Ar being released at slightly higher temperatures of between 600 and 700 °C. N.B.: Abundances of both noble gas isotopes are normalised to sample weights.

as part of this stepped-combustion study recorded a total ^{21}Ne release for sample 12064 of 2.94E−07 cc/g^{-1}, (Run 1), and 4.22E−07 cc/g^{-1} (Run 2), of which around 98% (2.88E−07 cc/g^{-1}) and 86% (3.61E−07 cc/g^{-1}), respectively, is of cosmogenic origin. Taking an average of both of these runs for sample 12064, a cosmogenic ^{21}Ne abundance of 3.25E−07 cc/g^{-1} is obtained, which is almost identical to the published abundance data.

This correlation is a useful check, confirming the reliability and stability of this stepped combustion method, as described above, across a range of samples. Such a correlation between cosmogenic ^{15}N and exposure age also suggests that, while the abundance of ^{21}Ne is a well-known measure of cosmic ray exposure (CRE) age, the abundance of ^{15}N (released at temperatures above ~1000 °C) is also a useful exposure parameter.

5.4.3. Trapped noble gas isotopes

The release of radiogenic ^{4}He is correlated with a release of a trapped ^{20}Ne component in samples 12064 and 14053 only (Fig. 5), although interestingly, in samples 12040 and 70035, which do not show co-release of ^{20}Ne with ^{4}He, ^{20}Ne is released at higher temperatures and is correlated with the release of cosmogenic ^{21}Ne instead (Fig. 6).

One possible explanation for this unexpected variation in ^{20}Ne release profiles could be that the trapped ^{20}Ne component is introduced during sample preparation, when highly reactive fresh mineral surfaces are created during crushing, which can attract any atmospheric gases present. Any such terrestrial contaminant gases would be only weakly bound to the mineral surface and could be expected to be released at low temperature steps during analysis. Alternatively, the friction generated during sample crushing may cause local atomic level heating, and thus some grain surfaces may be annealed, trapping the weakly-bonded gas in the mineral sub-surface as an 'inclusion'; such pseudo-inclusions would then release the trapped gas only at higher temperatures, as the trapped component begins to diffuse out of the sample. Thus, it may be possible to release a terrestrial trapped Ne component at the same high temperature steps as cosmogenic ^{21}Ne. A similar explanation is proposed by Niedermann and Eugster (1992), who observed over 75% of the terrestrial noble gases incorporated during crushing of lunar anorthositic samples being released at temperatures above 600 °C. In their study, they attribute these high-release temperatures with noble gas fixing by strong chemisorptive bonding, or by trapping beneath the sample surface, due to mechanical and thermal energy supplied during the crushing process. However, this is merely a speculative explanation, and cannot be resolved at this stage using the data collected in this study.

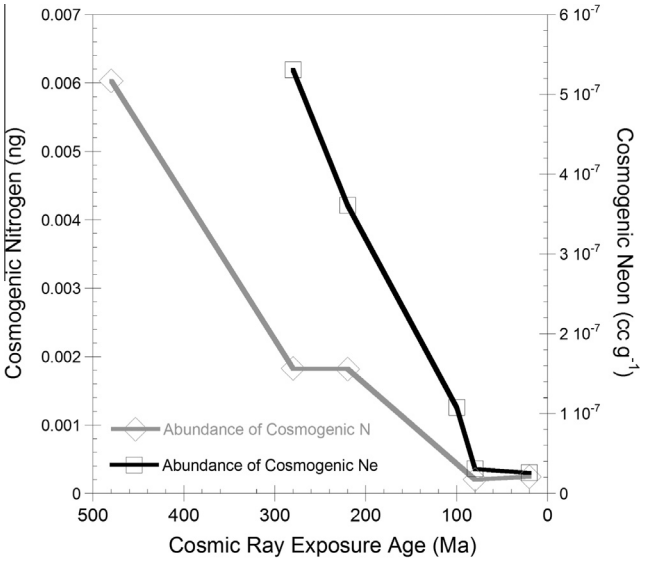

Fig. 4. Cosmogenic isotopes plotted against published calculated exposure ages. Data for cosmogenic ^{15}N is plotted in diamonds, and data for cosmogenic ^{21}Ne in squares.

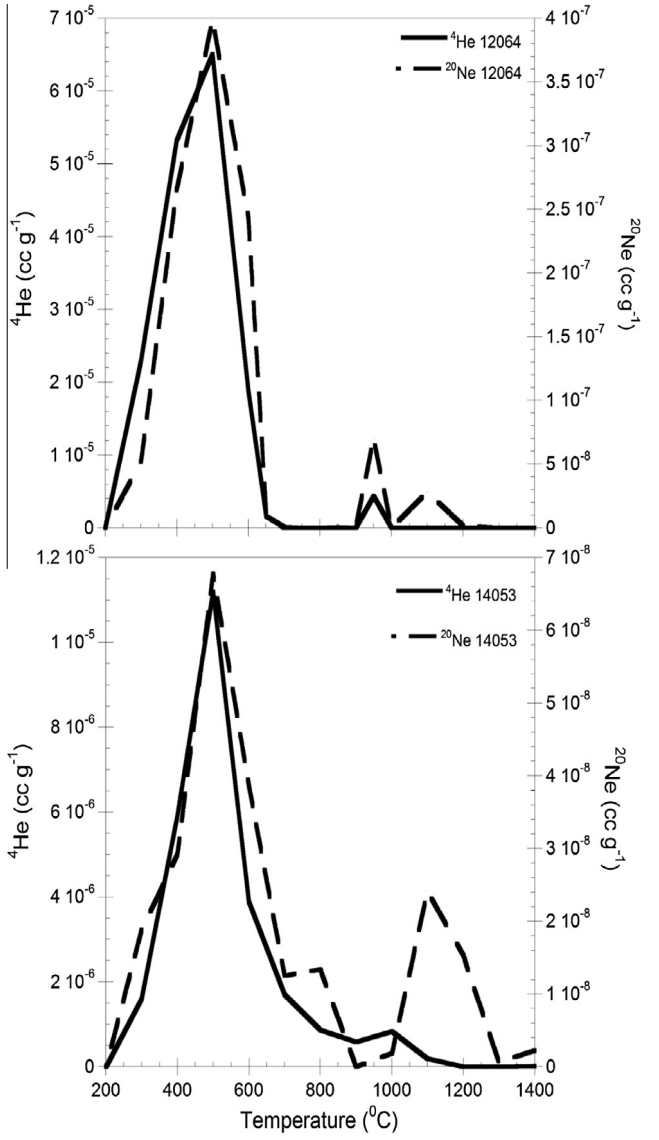

Fig. 5. Correlation between ^{4}He and ^{20}Ne in basalts 12064 and 14053. In these 2 samples, both the radiogenic ^{4}He component, and the trapped ^{20}Ne component are released at the same temperatures. However, in other basalt samples analysed, this is not the case. It is worth noting that ^{4}He is released at 500 °C across all of the samples analysed, and instead it is the release temperature of ^{20}Ne which is the unusual factor in these 2 samples. N.B.: Both noble gas isotope abundance data are normalised to sample weight, and the scales for the left and right axes vary between samples.

However, Ne isotope ratios in sample 12064,138 are an exceptional case (Table A5). After correcting both the ratios of ^{21}Ne/^{22}Ne and ^{20}Ne/^{22}Ne for contributions from a terrestrial atmospheric blank, and for the effect of mass fractionation within the mass spectrometer, a mixing trend between cosmogenic Ne and terrestrial atmospheric Ne is still observed. A second aliquot of 12064,138 (Run 2, sampled from the same bulk powder as Run 1) was analysed for Ne at a later date (approximately 6 months after Run 1), and again, these data display mixing between terrestrial atmospheric Ne and cosmogenic Ne after blank and mass fractionation corrections (see Fig. 7)

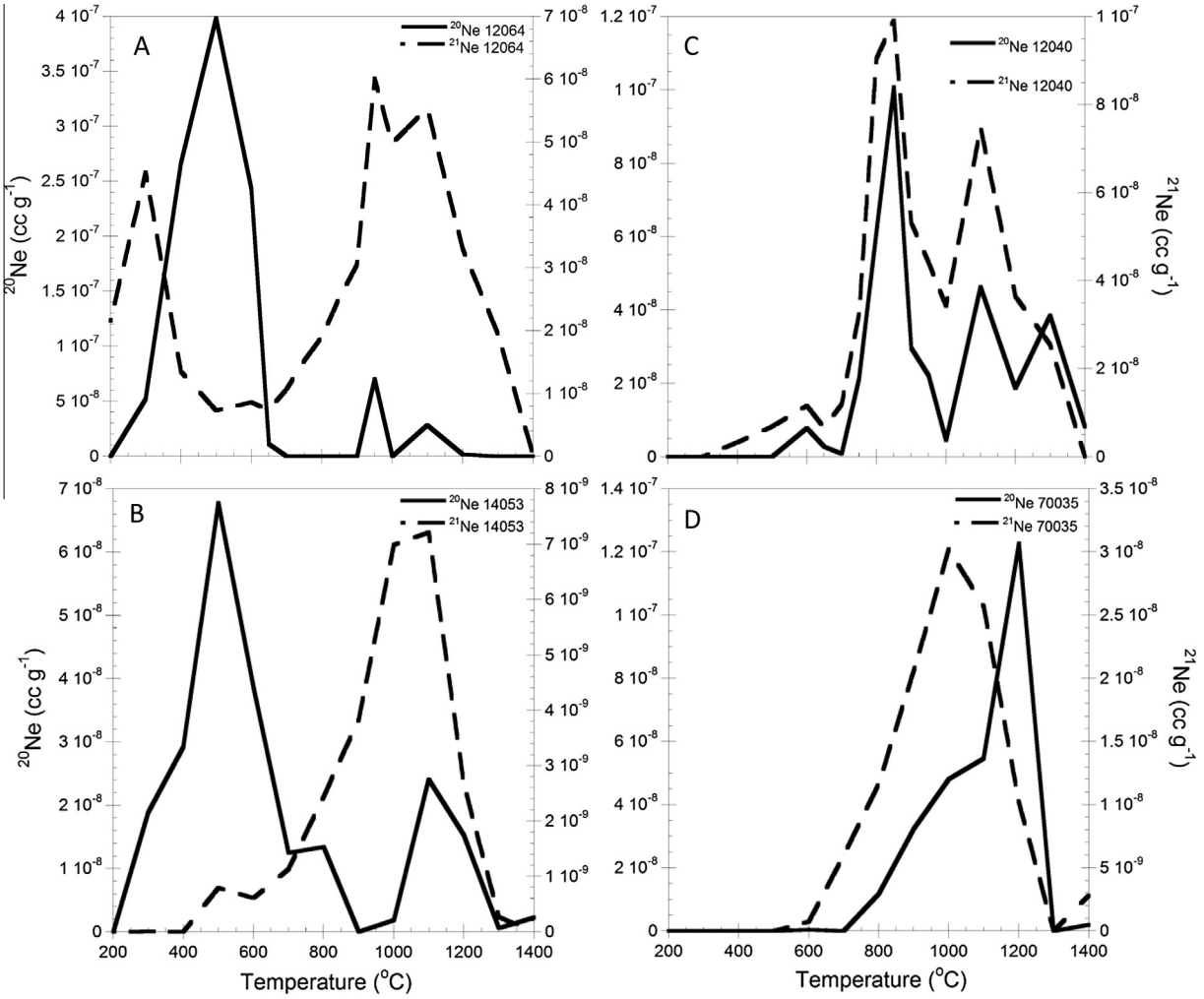

Fig. 6. ^{20}Ne and ^{21}Ne release profiles. For basalts 12064 and 14053 (plots A and B respectively), in which ^{20}Ne is co-released with ^{4}He at low temperatures, there is only a minor release of ^{20}Ne at higher temperatures (1000–1100 °C), correlated with the release of ^{21}Ne. However, in samples 12040 and 70035 (plots C and D respectively), where there is no correlation between ^{20}Ne and ^{4}He release patterns, both the trapped ^{20}Ne and the cosmogenic ^{21}Ne components are co-released at high temperatures. N.B.: Both noble gas isotope abundance data are normalised to sample weight, and the scales for the left and right axes vary between samples.

As discussed above, it is plausible that during sample crushing, terrestrial atmospheric gases were trapped in these samples, as observed by Niemeyer and Leich (1976), and Niedermann and Eugster (1992). This is supported by the fact that in all of the samples for which Ne data were collected in this study, trapped ^{20}Ne is observed in greater abundances than in previously published studies, despite good agreement between cosmogenic ^{21}Ne values. However, this trend is only observed in the blank-corrected Ne ratios in 12064, and not in any other sample. This is most likely due to the other samples in this study containing lower abundances of Ne, resulting in larger mass interference effects from doubly-charged CO_2 in the mass spectrometer. In 12064, this interference is minimal.

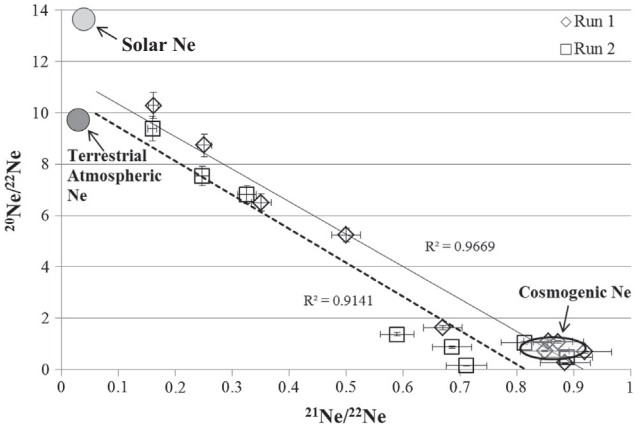

Fig. 7. Neon isotopic compositions within basalt 12064,138 (instrumental errors are 5%).

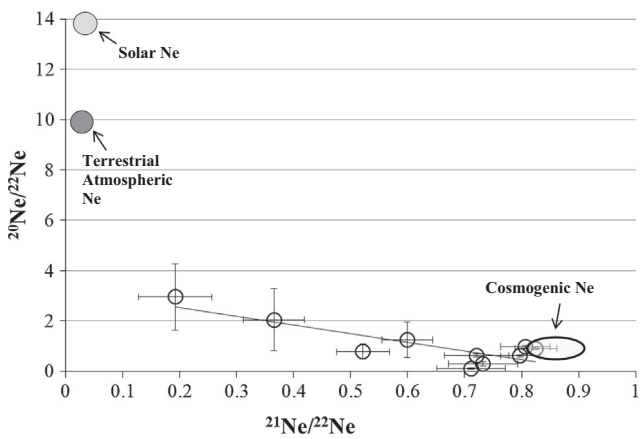

Fig. 8. Neon isotopic compositions within a chip of basalt 12064,140.

To resolve the issue of whether or not terrestrial Ne was incorporated into this sample during crushing, a separate chip of 12064 was analysed for He and Ne using the same protocols as described earlier, but this time without crushing the sample. A 5.725 mg chip of 12064,140 yielded almost identical results (for ^{4}He, $^{21}Ne_{cosm}$, and total ^{21}Ne abundance) as analyses of the crushed powder of 12064,138, and these data are also in excellent agreement with previous literature values (Table A7). However, in the chip of 12064,140, trapped ^{20}Ne was found to be an order of magnitude lower than in the crushed powder 12064,138. Further, Ne isotope ratios in the uncrushed sample do not show evidence of a component with a terrestrial-like composition (Fig. 8). Therefore, it does indeed appear that terrestrial atmospheric Ne was trapped in the powdered sample 12064,138 during crushing.

The other trapped noble gas for which data were collected is ^{36}Ar; again, as with any trapped atmospheric Ne, a higher abundance of ^{36}Ar might be expected if additional terrestrial atmospheric gases were introduced during sample crushing for this study. However, whilst a higher abundance of ^{36}Ar is observed in sample 14053 compared to published values, in most other samples in this study there is good agreement between these data and literature values, and in 12040, the amount of ^{36}Ar observed is lower than that measured in previous studies (Table A6).

Similarly, assuming that all of the trapped ^{20}Ne in 12064 was introduced during sample crushing and is therefore from the terrestrial atmosphere, a high abundance of N may also be expected, since N is many orders of magnitude more abundant in the terrestrial atmosphere than either Ne or Ar. By taking the relative abundances of N and Ne in the current terrestrial atmosphere ($N_2/^{20}$Ne = 65902.39 (by mass)), and applying that to the total abundance of trapped ^{20}Ne in sample 12064, the expected abundance of any trapped terrestrial N can be calculated (76494.09 ng of N for Run 1, or 62960.52 ng of N for Run 2). However, basalt 12064 releases only 42.52 ng of N, (between 1500 and 1800 times lower than the calculated expected abundance) and therefore, does not seem to show any evidence of significant trapped terrestrial atmospheric N, especially considering the fact that the majority of the N released in 12064 can be attributed (based on its C/N ratios (C/N = 72–171) and release temperatures) to terrestrial organic material and not the terrestrial atmosphere. Discounting the terrestrial organic N contribution, the measured abundance of N in 12064 is significantly lower than the expected contribution from contamination by terrestrial atmospheric N.

Thus, although these Ne data do support the addition of terrestrial atmospheric gases during sample crushing, Ar and N data do not. This is unexpected, as ^{36}Ar and N_2 are more abundant in the terrestrial atmosphere than ^{20}Ne and so would be expected to be trapped in greater abundance. Clearly, the effect of sample crushing on the addition of terrestrial gases is a complex process, and requires further investigation.

6. Conclusions

The simultaneous measurement of five different element abundances and isotopic data from the same aliquot of sample, combined with the high-temperature-resolution stepwise combustion used in this study, permit a truly in-depth analysis of the various volatile components present in six lunar basalt samples.

From the wealth of data collected, two separate stories emerge, one concerning the indigenous C and N contents of the Moon's interior, and the second revealing the later production of volatiles through extra-lunar processes acting on the samples during their time on the lunar surface.

Disregarding data from temperature steps dominated by terrestrial contaminants and by cosmogenic isotope overprinting, an isotopic signature of indigenous lunar N in basalts is revealed. With an average δ^{15}N value of around +0.35‰ (±9.11‰ (2σ)), this indigenous signature fits (within error) with the limited previous reports of indigenous lunar N, and indigenous N values for individual samples suggest a heterogeneous N abundance and isotopic signature within the lunar mantle.

The average C/N ratio of the indigenous lunar volatile component falls within the same range (C/N = 4–21) across all of the samples analysed in this study; this relatively tight range of values is consistently much lower and therefore distinct from the C/N ratios of terrestrial depleted mantle or the bulk-silicate Earth, highlighting the greater differentiation of Earth's mantle volatile signatures due to tectonic recycling of material when compared to the Moon, and the effect of differing oxygen fugacity on the degassing of C and N between the two bodies.

Cosmogenic N isotopes, similar to noble gas isotopes, present in the samples document the post-crystallisation exposure history of the mare basalts on the lunar surface.

The measurements of cosmogenic isotope abundances in this study are well correlated with calculated noble gas exposure ages

Table A1
Stepped combustion nitrogen release data for lunar basalts analysed in this study (– = not measured; † = blank level). N.B.: High temperature steps containing cosmogenic N have no error reported, since error propagation on such small abundances gives unrealistic uncertainties. However, these high temperature isotopic signatures have been used to calculate cosmogenic N abundances, and these correlate well with reported exposure ages, suggesting that these isotopic data, although associated with very large errors, are fairly reliable.

Temperature step (°C)	10017		12040		12064		14053		15555		70035	
	N (ng)	δ^{15}N (‰)	N (ng)	δ^{15}N (‰)	N (ng)	δ^{15}N (‰)	N (ng)	δ^{15}N (‰)	N (ng)	δ^{15}N (‰)	N (ng)	δ^{15}N (‰)
200	1.36	−7.09 ± 0.66	0.15	−3.29 ± 7.88	10.86	2.98 ± 0.34	4.48	−9.20 ± 0.71	0.98	−5.72 ± 0.99	4.23	−6.44 ± 1.19
300	3.41	−1.94 ± 0.51	5.73	1.03 ± 0.36	15.67	12.77 ± 0.42	10.48	−3.12 ± 0.30	8.82	15.47 ± 0.41	10.49	1.21 ± 0.29
400	0.20	−7.98 ± 26.84	3.50	11.26 ± 0.53	6.28	3.28 ± 0.45	6.82	−1.97 ± 0.45	1.34	26.18 ± 0.97	5.94	1.12 ± 0.47
500	†	1.69 ± 60.90	0.51	−8.13 ± 3.18	2.23	3.95 ± 0.63	8.15	0.80 ± 0.36	0.44	−0.34 ± 1.64	2.64	−0.82 ± 1.04
600	0.16	1.51 ± 36.68	0.91	−3.66 ± 1.31	1.75	5.11 ± 0.79	2.21	4.50 ± 1.21	0.93	1.05 ± 0.79	1.05	15.76 ± 2.49
650	–	–	0.40	−13.41 ± 5.67	1.11	−6.40 ± 0.91	–	–	0.75	−0.94 ± 1.02	–	–
700	0.48	3.41 ± 5.90	0.61	−6.80 ± 2.09	1.27	−1.80 ± 0.79	2.22	7.72 ± 1.21	0.73	2.30 ± 1.02	1.58	18.45 ± 1.68
750	–	–	0.97	−5.66 ± 1.34	1.05	−2.78 ± 0.98	–	–	0.41	0.64 ± 1.69	–	–
800	0.53	14.85 ± 10.38	0.52	21.90 ± 4.87	0.59	3.70 ± 1.62	1.46	−14.27 ± 1.82	0.39	7.01 ± 2.57	1.29	6.51 ± 2.10
850	–	–	0.43	49.43 ± 13.64	0.42	16.13 ± 3.87	–	–	0.08	1.73 ± 8.27	–	–
900	0.17	42.01	†	70.07	†	71.40	0.12	4.63 ± 23.91	0.05	−5.30 ± 63.73	0.49	6.57 ± 5.21
950	–	–	0.01	125.81	0.62	135.66	–	–	0.04	−1.93 ± 55.21	–	–
1000	0.22	179.08	†	120.42	0.16	517.78	0.70	−7.22 ± 3.88	0.04	2.91 ± 37.27	†	53.83
1100	0.21	604.83	0.13	458.89	0.12	731.58	0.58	41.69	0.74	22.07	†	123.03
1200	0.51	882.24	0.09	456.80	0.13	631.58	0.43	48.71	0.41	52.88	†	201.81
1300	0.16	1054.82	0.75	429.46	0.25	695.70	0.06	38.56	0.03	306.06	†	224.46
1400	0.02	174.21	†	60.96	0.01	61.77	0.14	−7.82	†	113.64	†	319.84

found in the literature, and they detail the build-up of cosmogenic isotopes, produced by spallogenic reactions, in lunar surface material through time.

Ultimately, these findings contribute to ongoing investigations into the volatile inventory of the Moon, of both its interior and its surface, the former having implications for how the Moon (and by extension, the Earth) formed and evolved. Assessing the volatile budget of the lunar surface is of importance for any potential future human Solar System exploration, from the point of view of *in situ* resource utilisation; lunar surface volatiles potentially could be harvested to provide fuel and other consumables, using the Moon as a stepping stone to support long duration manned missions further out into space, as well as advancing scientific understanding of how volatiles are delivered to and formed on planetary surfaces, post-accretion.

Acknowledgments

The authors wish to thank Evelyn Füri and Sami Mikhail for constructive reviews that greatly improved the manuscript. Romain Tartèse is thanked for cross-checking various calculations presented in the manuscript and for lively discussions on the topic of lunar volatiles. We thank CAPTEM for allocation of lunar samples. JM thanks the Science and Technology Facilities Council (STFC) and The Open University for PhD studentship funding. This work has been partially funded by the STFC (Grant Number ST/I001298/1 to M.A.). This manuscript is dedicated to the memory of our co-author, Professor Colin Trevor Pillinger.

Appendix A

See Tables A1–A7.

Table A2
Stepped combustion carbon release data for lunar basalts analysed in this study (– = not measured, † = blank level). N.B.: High temperature steps containing cosmogenic C have no error reported, since error propagation on such small abundances gives unrealistic uncertainties.

Temperature step (°C)	10017		12040		12064		14053		15555		70035	
	C (ng)	δ^{13}C (‰)	C (ng)	δ^{13}C (‰)	C (ng)	δ^{13}C (‰)	C (ng)	δ^{13}C (‰)	C (ng)	δ^{13}C (‰)	C (ng)	δ^{13}C (‰)
200	199.31	−27.88 ± 0.27	93.09	−30.59 ± 0.16	513.51	−27.75 ± 0.19	206.38	−28.28 ± 0.30	36.85	−22.32 ± 0.21	237.38	−28.81 ± 0.18
300	446.39	−35.77 ± 0.23	594.65	−35.30 ± 0.30	795.44	−32.45 ± 0.29	434.21	−34.12 ± 0.21	118.10	−24.02 ± 0.39	642.96	−34.92 ± 0.40
400	285.72	−29.89 ± 0.36	805.40	−29.88 ± 0.21	591.19	−33.78 ± 0.18	403.48	−33.28 ± 0.36	146.87	−31.31 ± 0.28	379.68	−33.70 ± 0.49
500	361.04	−4.93 ± 1.25	288.02	−34.53 ± 0.46	463.25	−33.81 ± 0.25	332.98	−33.41 ± 0.36	149.84	−30.17 ± 0.24	364.67	−40.09 ± 1.28
600	153.86	−23.01 ± 0.62	147.77	−33.52 ± 0.47	166.94	−33.73 ± 0.28	267.54	−14.65 ± 0.56	114.95	−30.59 ± 0.34	170.98	−32.72 ± 0.78
650	–	–	9.33	−37.10 ± 0.60	20.77	−29.05 ± 0.64	–	–	81.98	−32.84 ± 0.46	–	–
700	14.09	−20.40 ± 0.54	6.39	−44.39 ± 0.90	12.78	−31.68 ± 0.96	9.86	−32.14 ± 0.29	100.08	−32.22 ± 0.34	0.81	−26.62 ± 0.35
750	–	–	2.65	−28.44 ± 0.29	10.36	−18.87 ± 1.49	–	–	106.43	−32.82 ± 0.28	–	–
800	10.10	−17.04 ± 2.39	2.65	−28.44 ± 0.29	4.93	−17.55 ± 3.17	4.80	−42.07 ± 1.05	84.72	−33.51 ± 0.44	12.94	−31.74 ± 0.49
850	–	–	5.15	−19.86 ± 0.50	2.08	−4.29 ± 7.43	–	–	46.85	−30.08 ± 0.28	–	–
900	2.80	−19.74 ± 18.48	0.32	−23.04	0.79	−24.06	0.11	−30.42 ± 245.72	20.55	−28.49 ± 0.27	5.90	−23.38 ± 0.27
950	–	–	0.11	−24.29	5.71	−22.89	–	–	8.61	−28.86 ± 0.23	–	–
1000	4.80	−3.78	0.20	−25.15	0.15	−23.68	3.94	−26.88 ± 0.72	4.53	−22.80 ± 0.42	9.59	−20.97
1100	4.08	15.77	0.22	−15.63	0.40	−18.59	3.28	−26.77	11.53	−24.70	59.32	−23.68
1200	2.97	64.36	0.24	−4.96	0.23	−15.73	2.01	−27.27	52.89	−30.00	10.77	−15.22
1300	0.02	5.81	0.85	8.38	0.26	−17.29	0.02	−33.02	6.76	−25.31	7.25	−20.51
1400	†	−23.49	0.14	−31.09	0.30	−32.69	0.02	−34.64	2.29	−29.89	1.31	−29.48

Table A3
Stepped combustion helium release data for lunar basalts analysed in this study (– = not measured, nd = not detected).

Temperature step (°C)	10017 ^{4}He (cc g^{-1})	12040 ^{4}He (cc g^{-1})	12064 ^{4}He (cc g^{-1})	14053 ^{4}He (ccg^{-1})	15555 ^{4}He (cc g^{-1})	70035 ^{4}He (ccg^{-1})
200	–	nd	nd	2.23E−09	4.12E−08	nd
300	–	3.68E−06	2.28E−05	1.59E−06	2.51E−06	6.77E−06
400	–	1.44E−05	5.32E−05	5.91E−06	6.77E−06	2.39E−05
500	–	3.67E−05	6.51E−05	1.12E−05	1.49E−05	4.35E−05
600	–	2.67E−05	1.89E−05	3.89E−06	9.66E−06	1.89E−05
650	–	3.97E−06	1.62E−06	–	2.27E−06	–
700	–	1.64E−06	1.45E−07	1.70E−06	1.16E−06	6.86E−06
750	–	8.51E−07	nd	–	9.53E−07	–
800	–	7.37E−07	nd	8.71E−07	7.10E−07	4.01E−06
850	–	2.36E−06	7.88E−08	–	6.04E−07	–
900	–	4.84E−07	1.37E−08	5.84E−07	2.75E−07	3.86E−06
950	–	9.96E−07	4.38E−06	–	nd	–
1000	–	1.41E−06	nd	8.35E−07	nd	5.25E−06
1100	–	1.24E−07	nd	1.90E−07	nd	2.24E−06
1200	–	nd	nd	nd	nd	3.38E−06
1300	–	nd	nd	nd	2.12E−07	nd
1400	–	nd	nd	1.45E−08	nd	nd
Total		9.40E−05	1.66E−04	2.68E−05	4.01E−05	1.19E−04
Literature values	4.91E−04[a] 4.98E−04[b]	7.60E−05[c]	1.81E−04[a]	3.18E−04[d]	8.97E−05[d]	

[a] Taken from Hintenberger et al. (1971).
[b] From Huneke et al. (1972).
[c] From Eugster et al. (1984a).
[d] From Husain et al. (1972).

Table A4
Stepped combustion neon release data for lunar basalts analysed in this study (– = not measured, nd = not detected).

Temperature step (°C)	10017		12040		12064 Run 1		12064 Run 2		14053		15555		70035	
	^{20}Ne (cc g^{-1})	^{21}Ne (cc g^{-1})	^{20}Ne (cc g^{-1})	^{21}Ne (cc g^{-1})	^{20}Ne (cc g^{-1})	^{21}Ne (cc g^{-1})	^{20}Ne (cc g^{-1})	^{21}Ne (cc g^{-1})	^{20}Ne (cc g^{-1})	^{21}Ne (cc g^{-1})	^{20}Ne (cc g^{-1})	^{21}Ne (cc g^{-1})	^{20}Ne (cc g^{-1})	^{21}Ne (cc g^{-1})
200	–	–	nd	nd	nd	3.65E−09	1.52E−11	2.15E−08	nd	nd	nd	nd	nd	nd
300	–	–	nd	nd	9.52E−08	3.74E−08	5.19E−08	4.52E−08	1.89E−08	5.81E−12	nd	nd	nd	nd
400	–	–	nd	3.26E−09	2.83E−07	1.40E−08	2.66E−07	1.35E−08	2.92E−08	nd	nd	nd	nd	nd
500	–	–	nd	6.91E−09	3.60E−07	4.46E−09	3.98E−07	7.29E−09	6.78E−08	7.95E−10	nd	nd	nd	nd
600	–	–	7.79E−09	1.16E−08	2.15E−07	4.76E−09	2.44E−07	8.62E−09	3.87E−08	6.09E−10	nd	nd	4.23E−10	7.30E−10
650	–	–	2.74E−09	6.60E−09	–	–	1.11E−08	7.35E−09	–	–	nd	nd	–	–
700	–	–	8.52E−10	1.19E−08	1.86E−07	1.60E−08	nd	1.07E−08	1.25E−08	1.13E−09	nd	nd	nd	5.99E−09
750	–	–	2.13E−08	3.24E−08	–	–	nd	1.52E−08	–	–	nd	nd	–	–
800	–	–	6.14E−08	9.04E−08	1.90E−08	1.67E−08	nd	1.90E−08	1.34E−08	2.44E−09	nd	nd	1.17E−08	1.16E−08
850	–	–	1.01E−07	9.91E−08	–	–	nd	2.52E−08	–	–	nd	6.42E−10	–	–
900	–	–	2.96E−08	5.33E−08	2.43E−08	3.26E−08	nd	3.05E−08	nd	3.83E−09	nd	5.02E−09	3.24E−08	2.06E−08
950	–	–	2.21E−08	4.41E−08	–	–	7.03E−08	6.01E−08	–	–	nd	9.35E−09	–	–
1000	–	–	4.50E−09	3.43E−08	8.19E−08	6.75E−08	nd	4.98E−08	1.82E−09	6.99E−09	nd	6.87E−09	4.81E−08	3.02E−08
1100	–	–	4.64E−08	7.48E−08	3.50E−08	5.33E−08	2.84E−08	5.54E−08	2.41E−08	7.21E−09	nd	9.07E−09	5.46E−08	2.57E−08
1200	–	–	1.87E−08	3.64E−08	1.82E−10	2.79E−08	1.79E−09	3.30E−08	1.53E−08	2.66E−09	nd	nd	1.23E−07	1.02E−08
1300	–	–	3.86E−08	2.55E−08	nd	1.61E−08	nd	1.95E−08	5.78E−10	2.66E−10	nd	nd	nd	nd
1400	–	–	8.17E−09	nd	nd	nd	nd	1.84E−10	2.26E−09	nd	nd	nd	2.00E−09	2.79E−09
Total			3.63E−07	5.31E−07	1.30E−06	2.94E−07[*]	1.07E−06	4.22E−07[**]	2.24E−07	2.59E−08		3.10E−08	2.72E−07	1.08E−07
Literature values	7.92E−07[a]	4.66E−07[a] 4.80E−07[b]	5.40E−08[c]	4.11E−07[c] 4.20E−07[e]	2.95E−07[a]	3.13E−07[a]	2.95E−07[a]	3.13E−07[a]	1.20E−07[d]	2.21E−08[d]	7.97E−07[d]	1.15E−07[d]		

[a] Taken from Hintenberger et al. (1971).
[b] From Huneke et al. (1972).
[c] From Eugster et al. (1984a).
[d] From Husain et al. (1972).
[e] From Bogard et al. (1971).
[*] Of which, $^{21}Ne_{cosm}$ = 2.88E−07 cc/g^{-1}.
[**] $^{21}Ne_{cosm}$ = 3.61E−07 cc/g^{-1}.

Table A5
Neon isotope ratios for two aliquots of 12064,138. All ratios have been corrected for a blank contribution of terrestrial atmospheric composition, and for mass fractionation within the mass spectrometer (– = not measured, nd = not detected).

Temperature step (°C)	12064			
	Run 1		Run 2	
	$^{21}Ne/^{22}Ne$	$^{20}Ne/^{22}Ne$	$^{21}Ne/^{22}Ne$	$^{20}Ne/^{22}Ne$
200	nd	nd	0.71 ± 0.04	0.15 ± 0.01
300	0.67 ± 0.03	1.64 ± 0.08	0.69 ± 0.03	0.88 ± 0.04
400	0.35 ± 0.02	6.51 ± 0.33	0.33 ± 0.02	6.82 ± 0.34
500	0.16 ± 0.01	10.29 ± 0.51	0.16 ± 0.01	9.39 ± 0.47
600	0.25 ± 0.01	8.73 ± 0.44	0.25 ± 0.01	7.54 ± 0.38
650	–	–	0.59 ± 0.03	1.37 ± 0.07
700	0.50 ± 0.03	5.24 ± 0.26	nd	nd
750	–	–	nd	nd
800	0.86 ± 0.04	1.09 ± 0.05	nd	nd
850	–	–	nd	nd
900	0.85 ± 0.04	0.73 ± 0.04	nd	nd
950	–	–	0.81 ± 0.04	1.05 ± 0.05
1000	0.87 ± 0.04	1.07 ± 0.05	nd	nd
1100	0.92 ± 0.05	0.69 ± 0.03	0.89 ± 0.04	0.49 ± 0.02
1200	0.89 ± 0.04	0.26 ± 0.01	nd	nd
1300	nd	nd	nd	nd
1400	nd	nd	nd	nd

Table A6
Stepped combustion argon release data for lunar basalts analysed in this study (– = not measured, nd = not detected; ∗ = data not collected).

Temperature step (°C)	10017		12040		12064		14053		15555		70035	
	^{40}Ar (cc g^{-1})	^{36}Ar (cc g^{-1})	^{40}Ar (cc g^{-1})	^{36}Ar (cc g^{-1})	^{40}Ar (cc g^{-1})	^{36}Ar (cc g^{-1})	^{40}Ar (cc g^{-1})	^{36}Ar (cc g^{-1})	^{40}Ar (cc g^{-1})	^{36}Ar (cc g^{-1})	^{40}Ar (cc g^{-1})	^{36}Ar (cc g^{-1})
200	–	–	nd	8.56E−12	3.99E−07	7.39E−11	nd	nd	nd	1.39E−10	8.73E−11	2.42E−09
300	–	–	2.48E−07	3.12E−10	6.43E−07	nd	1.45E−06	7.38E−09	2.64E−07	nd	1.15E−06	nd
400	–	–	8.53E−07	2.01E−10	1.39E−06	2.85E−09	3.87E−06	1.30E−08	3.57E−07	3.02E−10	2.18E−06	4.19E−09
500	–	–	1.52E−06	6.32E−09	2.27E−06	1.41E−08	7.47E−06	1.70E−08	6.27E−07	1.10E−09	3.68E−06	3.38E−09
600	–	–	2.06E−06	1.07E−08	3.03E−06	2.98E−08	1.18E−05	2.52E−08	1.02E−06	5.19E−09	5.24E−06	5.64E−09
650	–	–	1.49E−06	5.84E−09	2.14E−06	2.24E−08	–	–	7.72E−07	4.00E−09	–	–
700	–	–	1.82E−06	7.91E−09	2.02E−06	2.96E−08	1.36E−05	3.32E−08	7.75E−07	2.48E−09	5.96E−06	5.78E−09
750	–	–	1.82E−06	8.08E−09	1.70E−06	3.60E−08	–	–	7.79E−07	3.73E−09	–	–
800	–	–	1.36E−06	5.39E−09	1.21E−06	2.46E−08	9.99E−06	2.93E−08	6.51E−07	3.39E−09	3.94E−06	3.42E−09
850	–	–	1.06E−06	3.88E−09	6.74E−07	1.15E−08	–	–	5.36E−07	2.80E−09	–	–
900	–	–	2.00E−07	nd	∗	∗	5.18E−06	1.56E−08	3.34E−07	5.71E−10	2.10E−06	2.46E−09
950	–	–	9.39E−08	nd	4.15E−07	5.34E−09	–	–	1.32E−07	1.05E−10	–	–
1000	–	–	8.59E−09	nd	nd	nd	3.58E−06	6.45E−09	nd	6.15E−10	6.73E−07	nd
1100	–	–	nd	3.37E−09	2.76E−08	9.91E−09	2.47E−06	5.72E−09	nd	4.77E−09	6.12E−07	5.37E−09
1200	–	–	nd	nd	2.61E−08	8.01E−09	1.61E−06	nd	nd	9.92E−09	1.26E−09	1.99E−10
1300	–	–	nd	nd	nd	nd	nd	nd	6.12E−09	2.08E−08	5.16E−09	nd
1400	–	–	8.34E−08	nd	2.18E−08	nd	nd	nd	6.55E−08	1.10E−09	2.37E−09	nd
Total			1.26E−05	5.20E−08	1.60E−05	1.94E−07	6.10E−05	1.53E−07	6.32E−06	6.10E−08	2.56E−05	3.29E−08
Literature values	4.95E−05[a]	4.65E−07[a]	9.90E−06[c]	1.48E−07[c]	1.65E−05[a]	1.91E−07[a]	6.42E−05[d]	4.98E−08[d]	9.13E−06[d]	1.85E−07[d]	1.53E−05[g]	8.41E−08[g]
	4.79E−05[b]			2.20E−07[h]				3.00E−08[f]	7.32E−06[e]	9.11E−08[e]		

[a] Taken from Hintenberger et al. (1971).
[b] From Huneke et al. (1972).
[c] From Eugster et al. (1984a).
[d] From Husain et al. (1972).
[e] From York et al. (1972).
[f] From Eugster et al. (1984b).
[g] From Stettler et al. (1973).
[h] From Bogard et al. (1971).

Table A7
Stepped combustion neon release data for 5.725 mg lunar basalt chip 12064,140 (nd = not detected).

Temperature step (°C)	12064,140			
	^{20}Ne (cc g^{-1})	^{21}Ne (cc g^{-1})	^{21}Ne/^{22}Ne	^{20}Ne/^{22}Ne
200	nd	nd	nd	nd
300	nd	5.65E−09	nd	nd
400	5.72E−08	2.55E−08	0.60 ± 0.04	1.25 ± 0.71
500	3.08E−08	1.83E−08	0.52 ± 0.05	0.78 ± 0.30
600	4.05E−08	6.76E−09	0.37 ± 0.05	2.05 ± 1.24
650	nd	1.64E−09	nd	nd
700	3.08E−08	1.89E−09	0.19 ± 0.06	2.95 ± 1.33
750	nd	4.02E−09	nd	nd
800	nd	7.84E−09	nd	nd
850	nd	1.87E−08	nd	nd
900	9.17E−09	2.48E−08	0.73 ± 0.06	0.30 ± 0.07
950	1.43E−09	2.02E−08	0.71 ± 0.06	0.11 ± 0.03
1000	1.89E−08	2.45E−08	0.72 ± 0.06	0.63 ± 0.07
1100	5.27E−08	4.76E−08	0.81 ± 0.04	0.97 ± 0.05
1200	5.17E−08	7.58E−08	0.80 ± 0.03	0.61 ± 0.03
1300	8.48E−08	8.59E−08	0.83 ± 0.04	0.90 ± 0.04
1400	nd	1.19E−09	nd	nd
Total	3.78E−07	3.70E−07*		
Literature values	2.95E−07[a]	3.13E−07[a]		

[a] Taken from Hintenberger et al. (1971).
* Of which, $^{21}Ne_{cosm}$ = 3.65E−07 cc/g^{-1} (98.5% of total ^{21}Ne released).

References

Abernethy, F.A.J., Verchovsky, A.B., Starkey, N.A., Anand, M., Franchi, I.A., Grady, M.M., 2013. Stable isotope analysis of carbon and nitrogen in angrites. Meteorit. Planet. Sci.. http://dx.doi.org/10.1111/maps.12184.

Becker, R.H., Clayton, R.N., Mayeda, T.K., 1976. Characterization of lunar nitrogen components. Proc. Lunar Sci. Conf. 7, 441–458.

Bogard, D.D., Funkhouser, J.G., Schaeffer, O.A., Zähringer, J., 1971. Noble has abundances in lunar material- cosmic-ray spallation products and radiation ages from the sea of tranquility and the ocean of storms. J. Geophys. Res. 76 (11), 2757–2779.

Boyce, J.W. et al., 2010. Lunar apatite with terrestrial volatile abundances. Nature 466 (7305), 466–469.

Boyd, S., Wright, I.P., Pillinger, C.T., 1997. Stepped-heating of carbonates and carbon-bearing quartz grains. Chem. Geol. 134, 303–310.

Burnett, D.S., Drozd, R.J., Morgan, C.J., Podosek, F.A., 1975. Exposure histories of Bench Crater rocks. Proc. Lunar Sci. Conf. 6, 2219–2240.

Cartigny, P., Jendrzejewski, N., Pineau, F., Petit, E., Javoy, M., 2001. Volatile (C, N, Ar) variability in MORB and the respective roles of mantle source heterogeneity and degassing: The case of the Southwest Indian Ridge. Earth Planet. Sci. Lett. 194, 241–257.

Chappell, B.W., Green, D.H., 1973. Chemical compositions and petrogenetic relationships in Apollo 15 mare basalts. Earth Planet. Sci. Lett. 18, 237–246.

Compston, W., Berry, H., Vernon, M.J., Chappell, B.W., Kay, M.J., 1971. Rubidium–strontium chronology and chemistry of lunar material from the Ocean of Storms. Proc. Lunar Sci. Conf. 2, 1471–1485.

Des Marais, D.J., 1978. Carbon, nitrogen and sulfur in Apollo 15, 16 and 17 rocks. Proc. Lunar Sci. Conf. 9, 2451–2467.

Des Marais, D.J., 1983. Light element geochemistry and spallogenesis in lunar rocks. Geochim. Cosmochim. Acta 47, 1769–1781.

Eberhardt, P. et al., 1974. Noble gas investigations of lunar rocks 10017 and 10071. Geochim. Cosmochim. Acta 38, 97–120.

Eugster, O., Eberhardt, P., Geiss, J., Grögler, N., Schwaller, H., 1984a. Cosmic ray exposure histories and ^{235}U–^{136}Xe dating of Apollo 11, Apollo 12, and Apollo 17 mare basalts. J. Geophys. Res. 89, C171–C181 (Proc. 15th Lunar Planet. Sci. Conf.).

Eugster, O. et al., 1984b. Cosmic ray exposure histories of Apollo 14, Apollo 15, and Apollo 16 rocks. J. Geophys. Res. 89, B498–B512 (Proc. 14th Lunar Planet. Sci. Conf.).

Evensen, N.M., Murthy, V.R., Coscio, M.R., 1973. Rb–Sr ages of some mare basalts and the isotopic and trace element systematics in lunar fines. Proc. Lunar Sci. Conf. 4, 1707–1724.

Friedman, I., Gleason, J.D., Hardcastle, K.G., 1970. Water, hydrogen, deuterium, carbon, and C^{13} content of selected lunar material. Proc. Lunar Sci. Conf., 1103–1109 (Apollo 11).

Friedman, I., O'Neil, J.R., Gleason, J.D., Hardcastle, K.G., 1971. The carbon and hydrogen content and isotopic composition of some Apollo 12 materials. Proc. Lunar Sci. Conf. 2, 1407–1415.

Friedman, I., Hardcastle, K.G., Gleason, J.D., 1972. Isotopic composition of carbon and hydrogen in some Apollo 14 and 15 lunar samples. J. Res. U.S. Geol. Survey 2 (1), 7–12.

Füri, E., Deloule, E., Gurenko, A., Marty, B., 2014. New evidence for chondritic lunar water from combined D/H and noble gas analyses of single Apollo 17 volcanic glasses. Icarus 229, 109–120.

Gast, P.W., Hubbard, N.J., Wiesmann, H., 1970. Chemical composition and petrogenesis of basalts from Tranquility Base. Proc. Lunar Sci. Conf., 1143–1163 (Apollo 11).

Gibson, E.K., Andrawes, F.F., 1978. Nature of the gases released from lunar rocks and soils upon crushing. Proc. Lunar Sci. Conf. 9, 2433–2450.

Gibson, E.K., Johnson, S.M., 1971. Thermal analysis-inorganic gas release studies of lunar samples. Proc. Lunar Sci. Conf. 2, 1351–1366.

Gopalan, K., Kaushal, S., Lee-Hu, C., Wetherill, G.W., 1970. Rb–Sr and U, Th–Pb ages of lunar materials. Proc. Lunar Sci. Conf., 1195–1206 (Apollo 11).

Greenwood, J.P., Itoh, S., Sakamoto, N., Warren, P., Taylor, L.A., Yurimoto, H., 2011. Hydrogen isotope ratios in lunar rocks indicate delivery of cometary water to the Moon. Nat. Geosci. 4, 79–82.

Halliday, A.N., 2013. The origins of volatiles in the terrestrial planets. Geochim. Cosmochim. Acta 105, 146–171.

Hauri, E.H., Weinreich, T., Saal, A.E., Rutherford, M.C., Van Orman, J.A., 2011. High pre-eruptive water contents preserved in lunar melt inclusions. Science 333, 213–215.

Hintenberger, H., Weber, H.W., Takaoka, N., 1971. Concentrations and isotopic abundances of the rare gases in lunar matter. Proc. Lunar Sci. Conf. 2, 1607–1625.

Horn, P., Kirsten, T., Jessberger, E.K., 1975. Are there Apollo 12 basalts younger than 3.1 b.y.? Unsuccessful search for A12 mare basalts with crystallization ages below 3.1 b.y.. Meteoritics 10, 417–418.

Hubbard, N.J., Gast, P.W., Rhodes, J.M., Bansal, B.M., Wiesmann, H., Church, S.E., 1972. Nonmare basalts: Part II. Proc. Lunar Sci. Conf. 3, 1161–1179.

Huneke, J.C., Podosek, F.A., Burnett, D.S., Wasserburg, G.J., 1972. Rare gas studies of the galactic cosmic ray irradiation history of lunar rocks. Geochim. Cosmochim. Acta 36, 269–301.

Husain, L., Schaeffer, O.A., Funkhouser, J., Sutter, J., 1972. The ages of lunar material from Fra Mauro, Hadley Rille and Spur Crater. Proc. Lunar Sci. Conf. 3, 1557–1567.

Javoy, M. et al., 2010. The chemical composition of the Earth: Enstatite chondrite models. Earth Planet. Sci. Lett. 293, 259–268.

Kaplan, I.R., Kerridge, J.F., Petrowski, C., 1976. Light element geochemistry of the Apollo 15 site. Proc. Lunar Sci. Conf. 7, 481–492.

Kerridge, J.F., Eugster, O., Kim, J.S., Marti, K., 1991. Nitrogen isotopes in the 74001/74002 double-drive tube from Shorty Crater, Apollo 17. Proc. Lunar Sci. Conf. 21, 291–299.

Libourel, G., Marty, B., Humbert, F., 2003. Nitrogen solubility in basaltic melt. Part I. Effect of oxygen fugacity. Geochim. Cosmochim. Acta 67 (21), 4123–4135.

Marti, K., Lightner, B.D., 1972. Rare gas record in the largest Apollo 15 rock. Science 175, 421–422.

Marty, B., 2012. The origins and concentrations of water, carbon, nitrogen and noble gases on Earth. Earth Planet. Sci. Lett. 313–314, 56–66.

Marty, B., Zimmermann, L., 1999. Volatiles (He, C, N, Ar) in mid-ocean ridge basalts: Assesment of shallow-level fractionation and characterization of source composition. Geochim. Cosmochim. Acta 63, 3619–3633.

Mathew, K.J., Marti, K., 2001. Lunar nitrogen: Indigenous signature and cosmic-ray production rate. Earth Planet. Sci. Lett. 184, 659–669.

McCubbin, F.M., Steele, A., Hauri, E.H., Nekvasil, H., Yamashita, S., Hemley, R.J., 2010. Nominally hydrous magmatism on the Moon. Proc. Natl. Acad. Sci. 107 (25), 11223–11228.

Moore, C.B., Gibson, E.K., Larimer, J.W., Lewis, C.F., Nichiporuk, W., 1970. Total carbon and nitrogen abundances in Apollo 11 lunar samples and selected achondrites and basalts. Proc. Lunar Sci. Conf., 1375–1382 (Apollo 11).

Moore, C.B., Lewis, C.F., Larimer, J.W., Delles, F.M., Gooley, R., Nichiporuk, W., 1971. Total carbon and nitrogen abundances in Apollo 12 lunar samples. Proc. Lunar Sci. Conf. 2, 1343–1350.

Moore, C.B., Lewis, C.F., Cripe, J.D., Delles, F.M., Kelly, W.R., Gibson, E.K., 1972. Total carbon, nitrogen and sulfur in Apollo 14 lunar samples. Proc. Lunar Sci. Conf. 3, 2051–2058.

Moore, C.B., Lewis, C.F., Gibson, E.K., 1973. Total carbon contents of Apollo 15 and 16 lunar samples. Proc. Lunar Sci. Conf. 4, 1613–1623.

Moore, C.B., Lewis, C.F., Cripe, J.D., 1974. Total carbon and sulfur contents of Apollo 17 lunar samples. Proc. Lunar Sci. Conf. 5, 1897–1906.

Murty, S.V.S., Goswami, J.N., 1992. Nitrogen, noble gases, and nuclear tracks in lunar meteorites MAC88104/105. Proc. Lunar Planet. Sci. Conf. 22, 225–237.

Niedermann, S., Eugster, O., 1992. Noble gases in lunar anorthositic rocks 60018 and 65315: Acquisition of terrestrial krypton and xenon indicating an irreversible adsorption process. Geochim. Cosmochim. Acta 56, 493–509.

Niemeyer, S., Leich, D.A., 1976. Atmospheric rare gases in lunar rock 60015. Proc. Lunar Sci. Conf. 7, 587–597.

Pearson, V.K., Sephton, M.A., Franchi, I.A., Gibson, J.M., Gilmour, I., 2006. Carbon and nitrogen in carbonaceous chondrites: Elemental abundances and stable isotopic compositions. Meteorit. Planet. Sci. 41 (12), 1899–1918.

Petrowski, C., Kerridge, J.F., Kaplan, I.R., 1974. Light element geochemistry of the Apollo 17 site. Proc. Lunar Sci. Conf. 5, 1939–1948.

Saal, A.E., Hauri, E.H., Cascio, M.L., Van Orman, J.A., Rutherford, M.C., Cooper, R.F., 2008. Volatile content of lunar volcanic glasses and the presence of water in the Moon's interior. Nature 454, 192–195.

Saal, A.E., Hauri, E.H., Van Orman, J.A., Rutherford, M.J., 2013. Hydrogen isotopes in lunar volcanic glasses and melt inclusions reveal a carbonaceous chondrite heritage. Science 340, 1317–1320.

Stettler, A., Eberhardt, P., Geiss, J., Grogler, N., Maurer, P., 1973. Ar^{39}/Ar^{40} ages and Ar^{37}/Ar^{38} exposure ages of lunar rocks. Proc. Lunar Sci. Conf. 4, 1865–1888.

Tartèse, R., Anand, M., Barnes, J.J., Starkey, N.A., Franchi, I., Sano, Y., 2013. The abundance, distribution, and isotopic composition of hydrogen in the Moon as revealed by basaltic lunar samples: Implications for the volatile inventory of the Moon. Geochim. Cosmochim. Acta 122, 58–74.

Thiemens, M.H., Clayton, R.N., 1983. Nitrogen contents and isotopic ratios of clasts from the enstatite chondrite Abee. Earth Planet. Sci. Lett. 62, 165–168.

Verchovsky, A.B., Fisenko, A.V., Semjonova, L.F., Pillinger, C.T., 1997. Heterogeneous distribution of Xenon-HL within presolar diamonds. Meteorit. Planet. Sci. 32, A131–A132.

Wasserburg, G.J., Papanastassiou, D.A., 1971. Age of an Apollo 15 mare basalt: Lunar crust and mantle evolution. Earth Planet. Sci. Lett. 13, 97–104.

Wasson, J.T., Kallemeyn, G.W., 1988. Compositions of chondrites. Phil. Trans. R. Soc. London A325, 535–544.

Wetzel, D.T., Rutherford, M.J., Jacobsen, S.D., Hauri, E.H., Saal, A.E., 2013. Degassing of reduced carbon from planetary basalts. Proc. Natl. Acad. Sci. 110 (20), 8010–8013.

Wright, I.P., Pillinger, C.T., 1989. C isotopic analysis of small samples by use of stepped-heating extraction and static mass spectrometry. In: Shanks, W.C., Criss, R.E. (Eds.), New Frontiers in Stable Isotopic Research: Laser Probes, Ion Probes and Small Sample Analysis. U.S. Geolog. Surv. Bull. 1890, pp. 9–34.

Wright, I.P., Boyd, S.R., Franchi, I.A., Pillinger, C.T., 1988. Determination of high precision N stable isotope ratios at the sub-nanomole level. J. Phys. E: Sci. Instrum. 21, 865–875.

York, D., Kenyon, W.J., Doyle, R.J., 1972. ^{40}Ar–^{39}Ar ages of Apollo 14 and 15 samples. Proc. Lunar Sci. Conf. 3, 1613–1622.